INSTITUTE OF PHYSICS PUBLISHING JOURNAL OF PHYSICS B: ATOMIC, MOLECULAR AND OPTICAL PHYSICS

J. Phys. B: At. Mol. Opt. Phys. **36** (2003) L319–L326 PII: S0953-4075(03)66141-9

LETTER TO THE EDITOR

Doubly excited states of helium observed in N- and l-specific partial photoionization cross-sections using lifetime-resolved fluorescence spectroscopy

James R Harries[1], James P Sullivan[1], Satoshi Obara[1], Peter Hammond[2] and Yoshiro Azuma[1,3]

[1] Photon Factory, IMSS, KEK, 1-1 Oho, Tsukuba 305-0081, Japan
[2] School of Physics, University of Western Australia, Crawley, Perth WA6009, Australia

E-mail: azuma@post.kek.jp

Received 14 July 2003
Published 12 September 2003
Online at stacks.iop.org/JPhysB/36/L319

Abstract

We have used a lifetime-resolved fluorescence technique to obtain the first measurements of partial photoionization cross-sections of ground state neutral helium with both N- and l-specific final ion state separation. Structure is observed in the He $4lnl'$ doubly excited state regions and the resulting resonance profiles and energy positions qualitatively compared to previously reported theoretical calculations. Due to the sensitive nature of the N- and l-specific partial cross-sections, states from the $(4, -2)_n$ series are observed for the first time.

The doubly excited states of helium have long been of interest since the first observations [1, 2] both experimentally and theoretically, particularly since becoming accessible to study in tunable photoexcitation with the advent of synchrotron radiation sources in the 1960s [3]. Most recently there have been very high resolution experimental studies of the doubly excited states observed in total ion yield [4–6] and fluorescence photon and metastable singly excited atom yield [7–10] and their photoexcitation and subsequent decay has also been investigated in an electric field [11]. A review of theoretical results is given by Tanner *et al* [12]. Most of the recent studies have concentrated on the states in Rydberg series which converge on the '$N = 2$' threshold, i.e. the threshold above which photoionization can produce He^+ in an excited state. There are $2N - 1$ 'optically allowed' $^1P^o$ series converging on each excited ion threshold of ion state principal quantum number N, and for the lowest $N = 2$ threshold all of these have been observed in photoion yield, VUV photon yield and metastable yield. Ultrahigh resolution measurements [9, 10] have also recently revealed the importance of triplet states. States converging on higher thresholds are more difficult to study since there are a larger number of

[3] Author to whom any correspondence should be addressed.

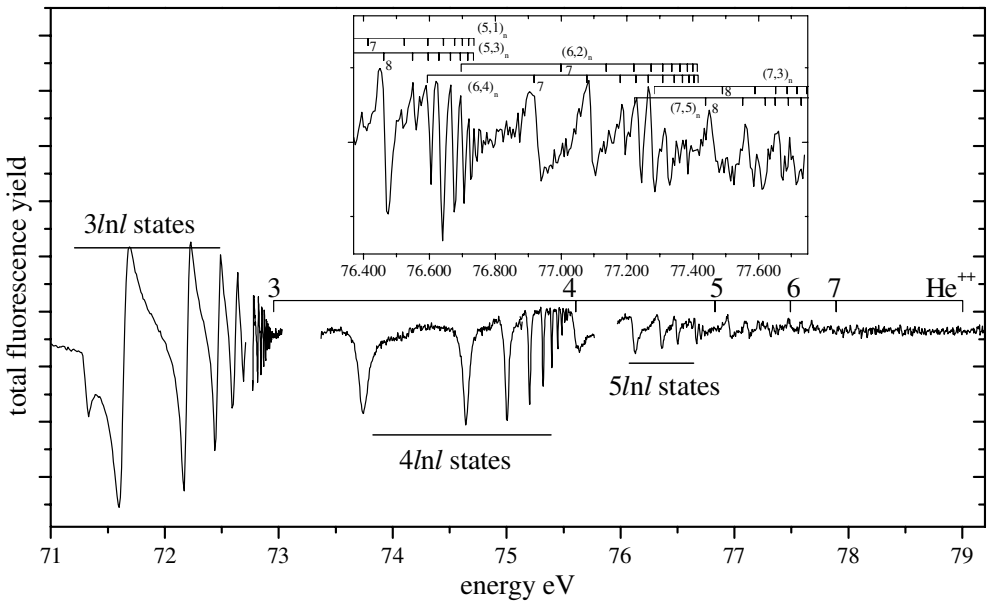

Figure 1. Total VUV fluorescence yield (see the text) from above the $N = 2$ threshold to the double ionization potential at 79 eV. The various data sets have been scaled and shifted to roughly preserve the observed relative yield. The inset shows a comparison with the theoretical energy positions of Rost *et al* [22] in the $N = 5$–7 doubly excited states region.

series (which begin to overlap at $N \approx 5$), and total ion yield measurements are hampered by the large ion yield due to direct ionization. This direct ionization, however, predominantly produces ions which are in the ground state and hence partial, final ion-state-specific photoionization yield measurements are more sensitive to the autoionization of doubly excited states. Recent experimental work (see [13–15] and references therein) detecting photoelectrons reports partial photoionization cross-sections, separating final ion states with different N. This photoelectron work, like recent theoretical approaches [16, 17], highlights the similarities of lineshapes for autoionizations where the change in N is the same.

We present measurements here where we detect the VUV fluorescence produced when the excited ion states decay. This method is inherently insensitive to photoionization to the ionic ground state and, as we show below, information about the partial ionization cross-sections can be obtained by a lifetime analysis of the fluorescence. Such an analysis can distinguish between final ion states not only of different N, but also of different orbital angular momentum quantum number l, something which is impossible to do using energy analysis of photoelectrons since the energy resolution available is insufficient to distinguish between the closely spaced final ion states of the same N but different l. The technique described here also has a large advantage over dispersed fluorescence methods, which would have a much reduced detection efficiency at the required resolution. A similar technique has been previously used to investigate the populations of H($3l$) produced in the photodissociation of H_2 [18] and electron impact of H [19], and also to probe H–H_2 collisions [20].

Figure 1 shows a selection of our total VUV fluorescence measurements over the region from the $N = 2$ threshold to above the double ionization limit. Similar measurements have been reported previously [21]. The various data sets have been scaled to roughly represent the actual relative yields, and the positions of some of the thresholds and doubly excited

state regions are shown. The inset to figure 1 shows a data set recorded at a resolution of approximately 5 meV in the region of the $N = 5$–7 doubly excited states, a region of interest due to the appearance of perturbing states from series converging on higher thresholds (see for example [14]). Also plotted are the theoretical energy positions of Rost *et al* [22] for selected series of states. Compared to the total photoionization measurements of Domke *et al* [4] the resonance profiles observed in fluorescence are different, and class-I series other than the $(N, N-2)$ series are much more prominent. Throughout this letter we use the simplified $(N, K)_n$ notation, where N and n represent the principal quantum numbers of the inner and outer electron and K is the angular correlation number used by Lin [23]. In the 'class-I, II, III' series groupings used by Rost *et al* [22] the doubly excited states are described as belonging to classes ordered by autoionization width; class-I series have the largest widths (e.g. the '+' series in the $N = 2$ states), followed by class-II series with characteristic widths one to two orders of magnitude lower. Class-II series are typified by the '$-$' series of $N = 2$ doubly excited states. Finally the class-III series are the most difficult to observe in photoionization measurements since they have characteristic widths a further two or more orders of magnitude smaller. The '2pnd' states belong to this class and, whereas the $N = 2$ class-I '+' and class-II '$-$' series were observed in the 1960s, the class-III 'nd' series could only be observed with the advent of millielectronvolt resolution in the 1990s.

It should be noted that the data shown in figure 1 are not *exactly* proportional to the total photoionization yield excluding He^+ ground state yield; also included is the signal due to the production of metastable singly excited states via VUV fluorescence decay and only a fraction of the 2s ion fluorescence is observed; these points are discussed further below. Also, for a detailed interpretation cascade pathways must be taken into account; our detector is only sensitive to VUV photons of energies above a few electronvolts.

In this letter we describe the further analysis of the data presented in figure 1 in the $N = 4$ doubly excited state region (73.3–75.6 eV) in which we separate out contributions due to the fluorescence of the 2s, 2p, 3s, 3p and 3d states. While earlier work by Woodruff and Samson [24] successfully separated the 2s and 2p ion state fluorescence using an electric field technique, to our knowledge this is the first use of a lifetime-analysis technique to separate out helium photoionization partial cross-sections.

The experiments were carried out at beamline 10.0.1 of the ALS (Advanced Light Source, Berkeley, USA) with preliminary measurements made at BL16B of the Photon Factory (Tsukuba, Japan). Helium gas from an effusive source was intersected by the photon beam, and a micro-channel plate (MCP) detector assembly directly faced the gas needle such that the detector was sensitive to VUV photons emitted perpendicular to the plane of polarization of the incoming radiation, and also to long-lived excited helium atoms with internal energy of over a few electronvolts. The direct detection of positive ions was suppressed by applying a few tens of volts to a mesh in front of the detector assembly, and electrons were repelled by the -2 kV applied to the MCP front plate. The electric field across the interaction region was limited to a few tens of volts per centimetre. The signal from the MCP was passed through a constant-fraction discriminator, and sent to the 'START' input of a TAC (time to amplitude convertor). The 'STOP' input was a pulse derived from the RF signals which regulate the synchrotron bunch structure, which in the ALS's two-bunch mode has a period of 328 ns. The TAC range was set to observe the whole 328 ns window between incoming light pulses; the output voltages were recorded with a multi-channel analyser and a fluorescence profile spectrum recorded for each incident photon energy step.

The timing signal in our detector consists of a prompt signal due to VUV fluorescence which appears on a timescale of 0–10 ns after a synchrotron radiation light pulse superimposed on a flat background of counts which appear time uncorrelated with the incoming light pulses.

This flat background has a number of components, including VUV fluorescence from states with lifetimes of the order of microseconds, and metastable helium atoms in long-lived (singly excited) states with internal energies of 19.8–24.6 eV. The prompt signal appears as the convolution of an 'instrument function' (which contains the shape and width in time (hundreds of picoseconds) of the synchrotron radiation pulse and the response function of our electronics) with exponential decay(s) due to the lifetimes of the fluorescing state(s).

Above the $N = 3$ threshold photoionization into the $N = 1$, 2 and 3 ion states is energetically allowed. The VUV photon signal consists of lifetime components from both the $N = 2$ (s, p) and 3 (s, p, d) states. All but the 2s state fluoresce preferentially directly to the ionic ground state with lifetimes ranging from 0.1 ns (2p) to 9.7 ns (3s). The 2s state is metastable with a lifetime of 2 ms. Although the 2s ions are travelling with thermal velocities and leave the field of view of the detector on a timescale of microseconds, our detection efficiency is enhanced by the weak electric field over the interaction region (up to a few tens of V cm^{-1}) and also by collisional de-excitation. Both of these effects are described by Woodruff and Samson [24] and references therein. In our timing spectra the 2s fluorescence signal thus appears in the flat time uncorrelated background. Also present in the flat background is a signal due to metastable atoms; however, this is only prominent very close to thresholds, where the density of states increases, autoionization rates decrease and metastable state production is strongly enhanced [14, 25].

The prompt fluorescence signal can be described by a linear superposition of components corresponding to each lifetime. Each component is the convolution of an instrument function with an exponential decay, which can be approximated by Gale's function [26] when the instrument function is approximated by a Gaussian lineshape. To obtain good fits to the data however we have found it necessary to use a measured instrument function, which we assume to be represented by the response of our system to the 0.1 ns 2p fluorescence, shown in the inset of figure 2. The main peak shape is approximately Gaussian, but is slightly asymmetric, with half-widths at half-maximum of 0.31 and 0.39 ns, much broader than the 2p fluorescence lifetime. Also visible are contributions from 'bunch impurities', where neighbouring bunches in the synchrotron ring have not been completely emptied of electrons during the filling process. While the signal from the largest of these bunches is around 300 times smaller than that from the main bunch (note the logarithmic scale of figure 2), it is necessary to include them in our analysis since in the tail of the exponential decay, short-lifetime (<1 ns) fluorescence from the rogue bunches can be of a similar magnitude to long-lifetime (>1 ns) fluorescence from the main bunch. In general this bunch structure is different from fill to fill of the synchrotron storage ring, and so an instrument function needs to be recorded for each data set.

The circular data points of figure 2 show a timing spectrum recorded at 74.1 eV—above the $N = 3$ threshold but below the $N = 4$ threshold. The dwell time for this data set was 8.5 s, and the data correspond to one of the points in the spectra shown in figure 3. The thick solid curve is a fit to the data with sums of convolutions of the instrument function with exponential decays corresponding to the fluorescence lifetimes of the 2p (0.1 ns), 3p (0.3 ns), 3d (0.97 ns) and 3s (9.7 ns) ion states. A very accurate measurement of the 2p lifetime is reported by Drake *et al* [27], and for the other lifetimes we have taken the lifetimes of the corresponding states in H adjusted for the helium ion [28]. Experimental values for some of the He^+ lifetimes are also available from beam–foil spectroscopy experiments [29, 30] and for the 2s state from a decay-in-flight experiment [31]. The individual contributions from the four separate states are plotted as thin solid curves in figure 3.

A rigorous analysis of our data should take into account cascade pathways. Cascade photons with sufficient energy can be detected, and we have assumed in our analysis that there is minimal detection efficiency for photons emitted in transitions between the excited ion states.

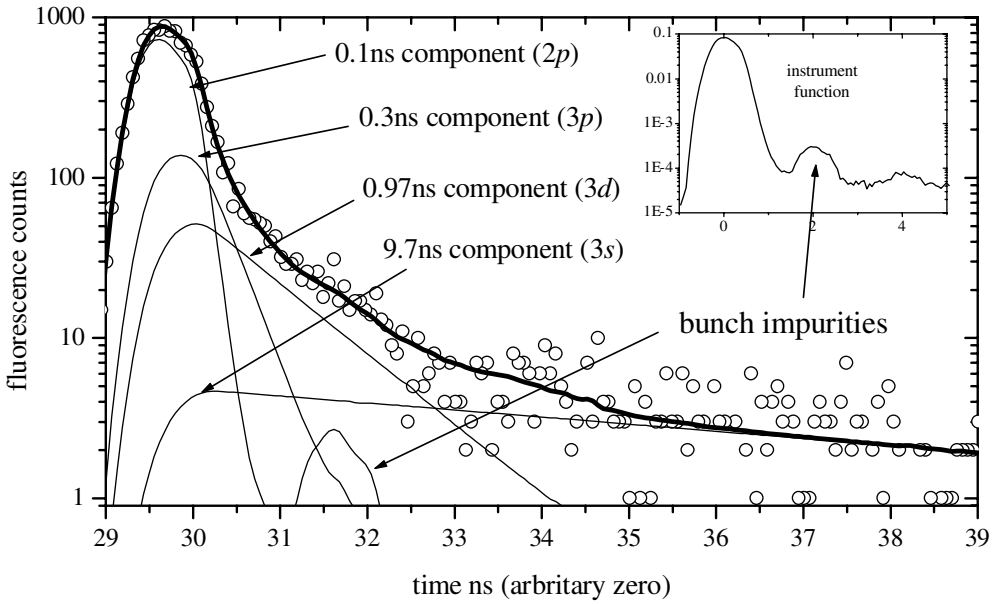

Figure 2. The timing spectrum above the $N = 3$ threshold showing the contribution of the $N = 3$ ion states. Solid curve: sum of four convolution functions; thin curves show the individual contributions. The small hump near 31.5 ns is a bunch impurity in the unconvolved instrument function, which is shown on its own in an inset.

The most important cascade contribution in this energy region is due to the 12% branching ratio of the 3p state to the 2s state. The decay photon is of too low an energy to be observed in our apparatus, but will produce a small component to our observed 2s yield. In the analysis presented here this and other contributions have been ignored, although for experiments at higher thresholds such analysis is likely to be essential.

We have recorded timing spectra at a range of energies between the $N = 3$ and 4 thresholds, covering the $N = 4$ doubly excited states region using an energy resolution of around 15 meV. At each energy point we have removed a flat background corresponding mainly to 2s fluorescence, and performed a fit to the remaining fluorescence profile to estimate the partial cross-sections. The fits are performed using a maximum-likelihood technique [32, 33], appropriate when the data are accurately represented by a Poisson distribution, as is the case for our spectra.

Figure 3 shows the results of fits to the timing spectra over the energy region of doubly excited states converging on the $N = 4$ ionization threshold. The graphs show two separate data sets: one above and one below 75.2 eV. The higher energy data set corresponds to a longer accumulation time, and hence the fits to the lifetime profiles are more precise. Above the $N = 4$ threshold at 75.6 eV the fitting procedure is no longer valid due to the contribution of $N = 4$ ion fluorescence—this is seen as a large step in the fitted yield of the 3s and 3d components. Also shown are the theoretical calculations of Sánchez and Martín [34] for each of the final ion state channels. Visible in the 2s fluorescence yield is a peak at the $N = 4$ threshold due to metastable state production, similar to the large peak observed below the $N = 2$ threshold [7, 9], and previously observed at this threshold by Sokell *et al* [35]. It is expected, however, that any metastable state production at doubly excited state energies below threshold would be unobservable on the background of 2s ion fluorescence. A method purely

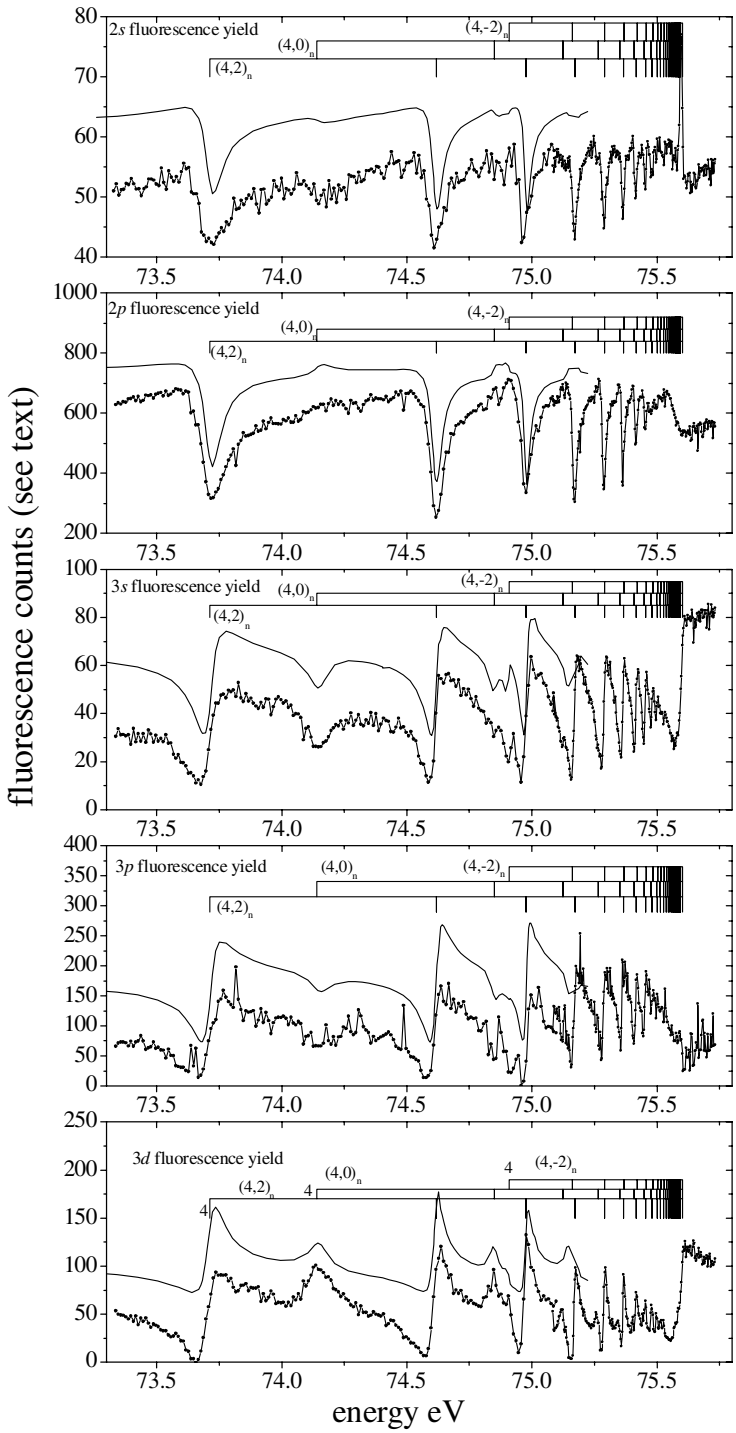

Figure 3. Resonances in the fluorescence yield due to doubly excited state autoionization: $N = 4$ states. Full curves show the calculations of Sánchez and Martín [34] and the theoretical energy positions of the three class-I series of Rost *et al* [22] are also shown.

sensitive to metastable singly excited atoms would require the quenching of the 2s state using an electric field or microwave field tuned to the 2s–2p transition to force the 2s ions to decay on a timescale similar to that of the 2p ion state fluorescence, thus clearing the timing window of VUV photon yield.

In the $N = 4$ doubly excited state region there are three 'class-I' [22] series, only two of which are observed in the total photoionization measurements of Domke *et al* [4]. Due to the sensitive nature of partial cross-section measurements all three series are visible in figure 3, including the previously unobserved $(4, -2)_n$ series. We see no evidence for the observation of the narrower class-II and class-III states, although higher quality data may reveal these states as resonances in the partial cross-sections.

The y-axes of figure 3 correspond to the magnitudes produced by the fitting procedure at each energy, and to some extent represent the relative partial cross-sections for production of the various final ion states. It should be noted that the statistical error in the partial cross-sections includes not only the contribution inherent to any counting experiment, but also that due to the fitting procedure. Due to the similarity in lifetime of the 2p and 3p states this fitting-procedure-related error is largest for the 3p trace. A more accurate determination of the relative yields will require more detailed analysis, accounting for cascade effects and relative detection efficiencies. In particular the detection efficiency of the 2s fluorescence is weakened by its long lifetime, as noted earlier.

In summary we have developed a technique for obtaining partial photoionization cross-sections by using lifetime-resolved fluorescence and applied it to measuring the partial photoionization cross-sections of helium in the $N = 3$ and 4 doubly excited states regions. We have observed states which are unobserved in total photoionization measurements. Further, more detailed experiments with higher resolution and/or improved statistical precision will enable a more accurate comparison with resonance parameters obtained from theory.

Extension of the technique to states converging on higher thresholds is in principle possible, but may be hampered by the high quality of the data required to accurately fit to the increasing number of lifetimes and cascade pathways. An alternative would be to combine our technique with either dispersing the fluorescence, or in-coincidence detection of energy-resolved scattered electrons.

This work was supported in part by a JSPS Grant-in-Aid for Scientific Research under category 'C', number 14540384. We would like to thank John Bozek, Nora Berrah, Bruce Rude and Alex Aguilar for help during beamtime, and are indebted to F Sánchez and I Martín for providing us with the results of their calculations. We are grateful to J G Lambourne for advice on the lifetime-fitting analysis. JPS acknowledges the support of the JSPS, PH that of AMRFP/ANSTO.

References

[1] Compton K T and Boyce J C 1928 *J. Franklin Inst.* **205** 497
[2] Kruger P G 1930 *Phys. Rev.* **36** 855
[3] Madden R P and Codling K 1963 *Phys. Rev. Lett.* **10** 516
[4] Domke M, Schulz K, Remmers G, Kaindl G and Wintgen D 1996 *Phys. Rev.* A **53** 1424
[5] Püttner R, Domke M, Grémaud B, Martins M, Schlacter A S and Kaindl G 1999 *J. Electron Spectrosc.* **101–103** 27
[6] Püttner R, Grémaud B, Delande D, Domke M, Martins M, Schlacter A S and Kaindl G 2001 *Phys. Rev. Lett.* **86** 3747
[7] Odling-Smee M K, Sokell E, Hammond P and MacDonald M A 2000 *Phys. Rev. Lett.* **84** 2598
[8] Rubensson J-E, Såthe C, Cramm S, Kessler B, Stranges S, Richter R, Alagia M and Coreno M 1999 *Phys. Rev. Lett.* **83** 947

[9] Penent F, Lablanquie P, Hall R, Žitnik M, Bučar K, Stranges S, Richter R, Alagia M, Hammond P and Lambourne J 2001 *Phys. Rev. Lett.* **86** 2758
[10] Gorczyca T W, Rubensson J E, Såthe C, Ström M, Agåker M, Ding D, Stranges S, Richter R and Alagia M 2000 *Phys. Rev. Lett.* **85** 1202
[11] Harries J R, Sullivan J P, Sternberg J B, Obara S, Suzuki T, Hammond P, Bozek J, Berrah N, Halka M and Azuma Y 2003 *Phys. Rev. Lett.* **90** 133002
[12] Tanner G, Richter K and Rost J M 2000 *Rev. Mod. Phys.* **72** 497
[13] Zubek M, King G C, Rutter P M and Read F H 1989 *J. Phys. B: At. Mol. Opt. Phys.* **22** 3411
[14] Sokell E, Wills A A, Comer J and Hammond P 1996 *J. Phys. B: At. Mol. Opt. Phys.* **29** L83
[15] Menzel A, Frigo S P, Whitfield S B and Caldwell C D 1996 *Phys. Rev.* A **54** 2080
[16] Schneider T, Liu C-N and Rost J-M 2002 *Phys. Rev.* A **65** 042715
[17] van der Hart H W and Greene C H 2002 *Phys. Rev.* A **66** 022710
[18] Terazawa N, Kouchi N, Ukai M, Kameta K and Hatano Y 1994 *J. Chem. Phys.* **100** 7038
[19] Williams J F and Mikozska A G 2003 *23rd Int. Conf. on Photonic Electronic and Atomic Collisions* unpublished
[20] Glass-Maujean M, Lauer S, Liebel H and Schmoranzer H 2000 *J. Phys. B: At. Mol. Opt. Phys.* **33** 4593
[21] Ström M, Såthe C, Ding D, Agåker M, Rubensson J-E and Gorczyca T W 2000 *ALS User Reports 2000*
[22] Rost J M, Schulz K, Domke M and Kaindl G 1997 *J. Phys. B: At. Mol. Opt. Phys.* **30** 4663
[23] Lin C D 1984 *Phys. Rev.* A **29** 1019
[24] Woodruff P R and Samson J A R 1982 *Phys. Rev.* A **25** 828
[25] Žitnik M, Bučar K and Štuhec M 2002 *Phys. Rev.* A **65** 032520
[26] Gale N H 1962 *Nucl. Phys.* **38** 252
[27] Drake G W F, Patel J and van Wijngaarden A 1983 *Phys. Rev.* A **28** 3340
[28] Wiese W L, Smith M W and Glennon B M 1966 *Atomic Transition Probabilities* vol 1 (Washington, DC: US Government Printing Office)
[29] Dotchin L W, Pegg D J and Chupp E L 1970 *Phys. Lett.* A **31** 85
[30] Lundin L, Oona H, Bickel W S and Martinson I 1970 *Phys. Scr.* **2** 212
[31] Kocher C A, Clendenin J E and Novick R 1972 *Phys. Rev. Lett.* **29** 615
[32] Hammond P 1996 *J. Phys. B: At. Mol. Opt. Phys.* **29** L231
[33] Lambourne J G *et al* 2003 *Phys. Rev. Lett.* **90** 153004
[34] Sánchez I and Martín F 1993 *Phys. Rev.* A **48** 1243
[35] Sokell E, Wills A A, Hammond P, MacDonald M A and Odling-Smee M K 1996 *J. Phys. B: At. Mol. Opt. Phys.* **29** L863